HHS Public Access

Author manuscript

Nat Struct Mol Biol. Author manuscript; available in PMC 2012 January 01.

Published in final edited form as:

Nat Struct Mol Biol. ; 18(7): 789–795. doi:10.1038/nsmb.2071.

Recognition of the F&H motif by the Lowe Syndrome protein OCRL

Michelle Pirruccello[1,2,3,5], **Laura E. Swan**[1,2,3,5], **Ewa Folta-Stogniew**[4], and **Pietro De Camilli**[1,2,3]

[1]Department of Cell Biology, Yale University School of Medicine, New Haven CT, 06510.

[2]Howard Hughes Medical Institute, Yale University School of Medicine, New Haven CT, 06510.

[3]Program in Cellular Neuroscience Neurodegeneration and Repair, Yale University School of Medicine, New Haven CT, 06510.

[4]W.M. Keck Biotechnology Resource Laboratory, Yale University School of Medicine, New Haven CT, 06510.

Abstract

Lowe syndrome and Type 2 Dent disease are caused by defects in the inositol 5-phosphatase OCRL. Most missense mutations in the OCRL ASH-RhoGAP domain found in affected patients abolish interactions with the endocytic adaptors APPL1 and Ses (both Ses1 and Ses2), which bind OCRL through a short F&H motif. Using X-ray crystallography, we have identified the F&H motif binding site on the RhoGAP domain of OCRL. We further show that clinical mutations affect F&H binding indirectly by destabilizing the RhoGAP fold. In contrast, a clinical mutation that does not perturb F&H binding and ASH-RhoGAP stability disrupts OCRL's interaction with Rab5. Additionally, OCRL's F&H binding site is conserved even in species that do not express APPL or Ses. Our study predicts the existence of other OCRL binding partners and demonstrates the critical role of the perturbation of OCRL interactions in disease.

Keywords

Endosome; Fanconi Syndrome; Clathrin; renal; trafficking

Mutations in OCRL are found in patients with the X-linked Oculo-Cerebral Renal Syndrome of Lowe (Lowe Syndrome)[1] and Dent disease[2]. Lowe Syndrome is characterized by renal tubular dysfunction, behavioral difficulties, developmental delay, and congenital

Correspondence should be addressed to P.D.C. (pietro.decamilli@yale.edu).

[5]These authors contributed equally to this work.

Accession codes

The coordinates have been deposited to the protein databank with the code 3QIS.

Author contributions

M.P., L.E.S., and P.D.C. designed research; M.P., L.E.S. and E.F.S. conducted experiments and contributed new reagents/analytical tools; M.P., L.E.S., and P.D.C. analyzed data; M.P. and P.D.C. wrote the paper.

cataracts[1, 3–6]. Dent disease patients have kidney defects similar to those of Lowe syndrome, but with no or mild associated defects, with the two disorders likely representing a phenotypic continuum[7,8].

OCRL belongs to the inositol 5-phosphatase family, a group of enzymes that dephosphorylate the 5' position of the inositol ring. In these enzymes, the catalytic core is typically delimited on either side by regions that specify the cellular localization and the distinct function of each enzyme. In OCRL the central 5-phosphatase domain, whose preferred substrates are PI(4,5)P_2 and PI(3,4,5)P_3, is flanked by an N-terminal PH domain and at the C terminus by an ASH (ASPM-SPD2-Hydin) domain followed by a catalytically inactive RhoGAP (Rho GTPase Activating) domain (Fig. 1a). The latter two domains are joined by a hydrophobic interface to form a single unit due to the stabilizing effect of each domain on the folding of the other. The same domain organization is shared by the related inositol 5-phosphatase INPP5B, which has a partially overlapping function with OCRL[9,10]. However, INPP5B is not associated with disease.

OCRL has a broad subcellular distribution. While originally considered a Golgi complex-associated protein[11–13], it was also subsequently shown to localize to multiple stations of the endocytic pathway, such as late-stage endocytic clathrin-coated pits and early endosomal sites[14–16]. This distribution is mediated by a variety of interactions, including the clathrin heavy chain (via two clathrin boxes located in loops of the PH domain and of the RhoGAP domain[14,15]), the clathrin adaptor AP-2 (via a motif adjacent to the PH domain [16]), with Rho family GTPases (via the RhoGAP domain[17]), and with Rab GTPases (via a site that, based on mutagenesis studies, is thought to involve portions of the ASH domain[18,19]). Additionally, the endocytic proteins APPL1 and Ses (both Ses1 and Ses2, referred to here as Ses1/2) are competitive interacting partners for the C terminus of OCRL[14,20,21], binding to OCRL via a short peptide stretch (11–13 amino acids long) that contains a phenylalanine and histidine motif termed the F&H motif [20]. Most of these interactions, with the exception of the interactions involving clathrin, are shared by INPP5B, consistent with genetic evidence for a partially overlapping function of OCRL and INPP5B[10].

In addition to the F&H motif, the APPL1 and Ses proteins share several features in that they possess a PH domain and an oligomerization surface[21]. APPL1, an adaptor protein comprising a BAR domain, a PH domain, and a PTB domain (Fig. 1a), is present on a subpopulation of peripheral PI(3)P-negative early endosomes[22,23]. Conversely, Ses (both Ses1 and Ses2), which contains a PH domain, a predicted coiled-coil, and an extended unfolded region (Fig. 1a), is localized on distinct intracellular vesicles including PI(3)P-positive classical early endosomes[20]. As endosomes mature, the more affine (for OCRL) Ses proteins displace APPL1[20], while OCRL remains associated with endocytic vesicles at both the APPL1 and Ses stage. The precise binding site for the F&H motif peptide in the ASH-RhoGAP domain of OCRL has not previously been mapped. It was shown, however, that F&H peptide binding requires the entire ASH-RhoGAP module[14,20].

The multiple localizations and interactions of OCRL are thought to help coordinate intracellular membrane traffic with changes in the phosphoinositide composition of associated membranes. Equally, OCRL may prevent ectopic or excessive accumulation of

$PI(4,5)P_2$ and $PI(3,4,5)P_3$ on intracellular membranes. Current models propose that a main function of OCRL is to regulate, via its action on membrane phosphoinositides, some aspect of endocytic and recycling membrane traffic. Such an action would explain, for example, the reabsorption defects in kidney proximal tubules that are characteristic of Lowe syndrome and Dent disease. Given the critical role of phosphoinositides in the regulation of several membrane proteins and of interactions between membranes and cytoplasmic proteins, spatial control of OCRL recruitment may be equally as important as its intrinsic catalytic activity. Hence, a precise understanding of OCRL interactions is crucial to the elucidation of mechanisms of disease.

While the majority of disease-causing mutations in OCRL result in lack of protein expression, major truncations and deletions, or missense mutations which directly impair catalytic activity, a group of missense mutations are found in the ASH-RhoGAP domain[3,20,24–30]. Cells derived from patients carrying these mutations possess reduced 5-phosphatase activity [31–33], a criteria for diagnosis, suggesting that mutations in the ASH-RhoGAP domain negatively impact some aspect of OCRL activity. Many of these missense mutations abolish interactions with F&H motif-containing proteins, while some other interactions are preserved (such as that with clathrin)[14,20,27]. When overexpressed, OCRL protein bearing these mutations has a primarily diffuse, cytosolic localization[20,27].

In order to elucidate the structural basis of the interaction between the ASH-RhoGAP domain and the F&H motif, we have solved the crystal structure of the ASH-RhoGAP domain of OCRL in complex with a 13-amino acid peptide from human Ses1 encompassing the F&H motif. The peptide has a predominantly helical conformation and binds to a well-conserved groove on the posterior surface of the RhoGAP domain. These results explain the importance of protein folding in the generation of this binding surface and provide a framework to explain the impact of patient mutations on ASH-RhoGAP domain interactions.

RESULTS

The ASH-RhoGAP domain in complex with the Ses1 F&H peptide

To understand the molecular details of the interaction between the ASH-RhoGAP domain of OCRL with the F&H motif, we solved the crystal structure of the OCRL ASH-RhoGAP in complex with the minimal OCRL binding peptide from Ses1 (residues 223–235) (Fig. 1a and 1b, and Table 1). As expected, the new structure of the ASH-RhoGAP domain was very similar to that solved previously[14], with differences in conformation primarily due to crystal packing interactions (Supplementary Fig. 1a and 1b). Importantly, in this crystal form electron density for the entire ASH domain was visible due to contacts with neighboring molecules in the lattice. This allowed for an improved definition of this domain, which is structurally most similar to the MSP domain family as judged by a Dali search[34] (Supplementary Fig. 2). This prompted the renaming of the ASH domain secondary structure elements according to the nomenclature previously adopted for VAP-A, a member of the MSP family[35]. While several MSP proteins oligomerize, the ASH domain of OCRL is not involved in oligomer formation, as the OCRL ASH-RhoGAP domain is monomeric in solution (Supplementary Fig. 3).

The fold of the RhoGAP domain in the new crystal structure was virtually identical to that of the previous structure, with an RMSD of 0.47 Å. However, due to crystal packing, there was no density for the long, clathrin box-containing loop observed in the previous structure. The ASH and RhoGAP domains are intimately connected to each other via a single alpha helix of the ASH domain that is arranged as a hinge between the two domains. The orientation of the ASH domain relative to the RhoGAP domain slightly differs between the two structures, due to a paddle-like motion centered on this hinge (Supplementary Fig. 1a).

The F&H peptide from Ses1 has clear electron density and adopts a helical conformation, as would be expected due to its heptad character (Fig. 1a and 1b). It is bound to the RhoGAP domain at a surface opposite to its interface with the ASH domain. To our knowledge, no other structurally characterized RhoGAP uses this surface for protein-protein interactions.

Interactions between the RhoGAP domain and the F&H peptide

The interface between the F&H motif and the RhoGap domain of OCRL is shown in detail in Fig. 1b. The F&H helix docks against the back of the RhoGAP domain in the groove formed between helices αA and αE, with the residues used in recognition of the F&H proteins highly specific for OCRL and INPP5B RhoGAP domains (Supplementary Fig. 4). The nominative phenylalanine is tucked into a hydrophobic pocket formed by Phe842 and Phe746 of OCRL, where the side chain of Phe746 has rotated to accommodate this interaction. There are additional hydrophobic contacts mediated by residues Val734, Tyr838, and Leu839 in OCRL and Phe2, Leu5 and Tyr9 in the Ses1 peptide. The importance of Leu5 is consistent with the evolutionary conservation of a hydrophobic residue at that position[20]. The histidine sidechain of the peptide hydrogen bonds to Asp743 of OCRL, and the main chain carbonyl of this residue hydrogen bonds with the indole nitrogen of Trp739.

The helical nature of the peptide is broken at position 11. This residue corresponds to the terminal proline in the minimal (11-mer) APPL1 F&H peptide (Fig. 1c), which is otherwise predicted to have a similar alpha-helical fold. Thus, the helical portion of the F&H motif is equivalent in both the APPL1 and Ses1/2 adaptor families. The remainder of the Ses1 peptide loops back around with Glu12 establishing a hydrogen bond with Lys691, a residue located at the base of the clathrin-binding loop, and Ile13 making further hydrophobic contacts with OCRL. The extra contacts mediated by these residues that are present in both Ses1 and Ses2, but not APPL1, likely accounts for the higher binding affinity of Ses1 and 2 for OCRL relative to APPL1 (Table 2).

In APPL1 there is a requirement for a serine in position 1 of the peptide (a proline in Ses1). Thus, although the core helical F&H binding mode is likely to be the same for the two proteins, there are small differences between the Ses peptides and the APPL1 peptide regarding contributions of the N- and C- terminal residues. Accordingly, mutation of the first proline in the Ses1 peptide to serine increases the affinity of the peptide to one similar to the more affine Ses2 peptide. The Ses2 F&H peptide has a cysteine rather than a proline at this position, perhaps explaining the increase in affinity (Table 2 and Fig. 1c). Attempts to co-crystallize the ASH-RhoGAP domain in complex with the APPL1 peptide were unsuccessful.

We previously identified a serine residue in APPL1 (Ser410) whose phosphorylation by PKA abolished the interaction with OCRL[14]. In addition, the first serine residue in the APPL1 F&H motif was also recently reported as a phosphorylation site[36]. We have now found by Surface Plasmon Resonance (SPR) that phosphorylated serines at either position in the APPL1 peptide severely interfere with the interaction of GST-tagged ASH-RhoGAP constructs (Table 2). The mechanism for this effect on binding is not clear from the structure, but may involve either a destabilization of the helical conformation of the peptide or charge repulsion from neighboring residues. The negative effect of the phosphorylation of the serine residue at the first position confirms the importance of this residue for APPL1 binding.

Mutational analysis of the F&H binding site

To validate the F&H binding surface in the ASH-RhoGAP domain, we engineered mutations in this domain expected to impact binding and tested them in biochemical assays and in living cells. Trp739 was mutated to alanine to perturb the hydrophobic surface while not affecting the stability of the protein (Fig. 1b). Additionally, we mutated Asp743 to the large, positively charged arginine. Both mutations disrupted binding of the F&H motif-containing protein, APPL1, but not clathrin, in GST pull downs from a rat brain extract using GST fusions of wild-type and mutant ASH-RhoGAP constructs as bait (Fig. 1d).

The OCRL^{W739A} mutation was further tested in a variety of assays. GST-pulldowns from COS-7 cells using fusions of APPL1 and Ses1 F&H peptides as bait showed binding of endogenous and transfected GFP-tagged OCRL^{WT}, but not of GFP-OCRL^{W739A} (Supplementary Fig. 5). Likewise, SPR experiments revealed binding of purified recombinant ASH-RhoGAP^{WT}, but not ASH-RhoGAP^{W739A}, to F&H peptides from APPL1 and Ses1/2 (Table 2 and Supplementary Fig 6).

To determine whether disruption of the F&H peptide interface on OCRL affected the colocalization of OCRL with APPL1 and Ses, GFP-OCRL^{WT} and GFP-OCRL^{W739A} were expressed in Lowe syndrome patient-derived fibroblasts[37]. The use of these cells allowed us to avoid potential artifacts due to competition with the endogenous enzyme. As shown in Figure 2, both GFP-OCRL^{WT} and GFP-OCRL^{W739A} had broad and similar distributions in vesicular structures throughout cells, with an additional concentration in the Golgi complex area that was variable from cell to cell. Furthermore, as described for WT cells[20,22], APPL1 localized to a peripheral subpopulation of endosomes, while Ses2 was localized on more centrally located organelles, primarily endosomes and vesicles in the Golgi complex area, in cells expressing GFP-OCRL^{WT}. Importantly, GFP-OCRL^{WT} colocalized with both APPL1 and Ses2 on these two populations of vesicles, whereas GFP-OCRL^{W739A} showed a substantial reduction in colocalization with either protein (78% reduction for APPL1 and 60% for Ses2, $P < 0.0001$). Interestingly, the overall localization of APPL1 on peripheral vesicles seemed to be similar in cells expressing GFP-OCRL^{WT} or GFP-OCRL^{W739A} (or even in the total absence of OCRL[14,27]), most likely due to the direct binding of APPL1 to the early endosomal Rab5[23,27,38]. In contrast, Ses2 was largely cytosolic when expressed in the absence of OCRL or when co-expressed with OCRL^{W739A}, thus indicating that its localization is critically dependent on OCRL.

These studies verify that the crystallographically identified F&H motif recognition surface is required for the colocalization of OCRL with F&H proteins on endosomal compartments. It will be interesting to determine whether OCRL^{W739A} can rescue defects observed in cells that lack OCRL. Such an analysis will require robust quantitative assays that so far have not been developed.

Conservation in the F&H binding site

Strong support for the physiological importance of the F&H binding site on the ASH-RhoGAP domain of OCRL comes from the high conservation of this site throughout evolution. When the amino acid sequences of 46 OCRL/INPP5B homologs were used to map the conservation of residues onto the surface of the ASH-RhoGAP structure, the F&H binding surface was one of two highly conserved sites (Fig. 3). This conservation was specific for the RhoGAP domain of OCRL/INPP5B proteins (Supplementary Fig. 4). Intriguingly, this interface is conserved in diverse lower organisms, such as Trypanosomes, that encode an OCRL/INPP5B homologue (Fig. 3), but neither APPL1 nor Ses1/2. This leads us to speculate that there may be other F&H proteins conserved throughout evolution that function in concert with OCRL. Surprisingly, the OCRL/INPP5B homologue in *Caenorhabditis elegans* (NP_001122420) does not contain the appropriate residues for interaction with F&H motif-containing proteins. This interaction may be lost, or the F&H motif binding site may have diverged or co-evolved with an F&H motif-containing protein.

Another highly conserved surface mapped onto the ASH domain (Fig. 3). Since mutations in this region affect Rab5 binding (reference[19] and see below), this surface likely represents the Rab binding site.

Impact of patient mutations on the ASH-RhoGAP domain

Most patient missense mutations in the ASH-RhoGAP domain result in loss of APPL1 or Ses1/2 binding[14,20,27]. However, none of these mutations map to the F&H binding site. As the bound F&H peptide is wedged between two helices on the OCRL RhoGAP domain, it follows that the interaction requires a folded domain.

Given the extensive contact between the two domains[14], it is clear that the stability of the ASH and RhoGAP domains are intertwined, such that destabilizing one will likely affect the stability of the other domain. Additionally, binding partners may help stabilize the conformation of the ASH-RhoGAP pair. For example, the tip of the ASH domain, which likely includes residues important for Rab binding (reference[19], and see below), is unstructured in the previous crystal structure, while stabilized here due to crystal packing interactions (Supplementary Fig. 1b). This difference could explain previous work showing the ability of some F&H binding defective mutants to recognize Rac1 and/or Rab5[14,27]. The folded G protein partners may be able to effectively compensate for the destabilization of the ASH-RhoGAP domain, whereas the short F&H motif is insufficient.

As the crystal structure reported here comprises the fully ordered ASH-RhoGAP unit, it provides us with the opportunity to precisely map the locations of all of the currently described missense mutations found in the ASH-RhoGAP domain, expanding the number of

mutations previously analyzed (ΔE585, A797P, and I768N)[14]. A common theme that emerges is the convergence of patient mutations onto specific regions of both the ASH and RhoGAP domains, pointing toward networks of amino acids likely to have a critical importance in maintaining stability.

In the ASH domain, deletion of Glu585 (ΔE585) was shown to alter affinity for both Rab5 and APPL1[14,20,27]. As discussed previously[14], this mutation disrupts the alternating hydrophobic/hydrophilic register of a β-sheet in the ASH domain, likely causing a global folding defect in the protein. Another mutation that impairs F&H binding, L634P, occurs at a residue located directly adjacent to Glu585 on a neighboring strand. The V577E mutation maps to the hydrophobic core of the ASH domain and mutation of valine to a charged amino acid would directly impinge on the stability of the two beta strands bearing Glu585 and Leu634 (Fig. 4).

A signature of the ASH domain family is an asparagine residue that is absolutely conserved in all ASH domains[39] (Supplementary Fig. 2). The disease-causing N591K mutation found in Lowe syndrome corresponds to this residue. Structurally, the sidechain of this residue is important for conferring the conformation of the tip of the ASH domain by forming multiple hydrogen bonds with residues in this region (Supplementary Fig. 7).

In the RhoGAP domain, Ile768 (I768N) stabilizes interactions between helices αA1 and αB, and is frequently a small, hydrophobic, side chain in related RhoGAPs (Supplementary Fig. 3 and reference[14]). Additionally, Leu891 (L891R[28]) in the αG helix is involved in hydrophobic packing, and changing this residue to a hydrophilic side chain would disrupt folding. Mutations A797P[14], P799L and P801L would all be detrimental to the proper folding of a region comprising the end of helix αB (A797P) and the following loop (P799L, P801L) where the proline residues impose a unique conformation. Helix αB contains components involved in recognizing Rho GTPases in related GAPs[40]. Additionally, these mutations cluster in the vicinity of residues 687 (L687P), 679 (C679W), and 737 (E737D)[30], which contact each other in the interior of the folded protein. Interestingly, this cluster includes a residue at the base of helix αA (Glu737). This helix contains residues that recognize the F&H motif directly, relating this amino acid network to the formation of the F&H binding site.

Consistent with a predicted defect in folding, recombinant ASH-RhoGAP constructs bearing patient mutations which disrupt F&H motif binding display dramatically enhanced degradation and co-purify with a greater amount of bacterial chaperone protein than the wild-type construct (Fig. 4). In contrast, ASH-RhoGAP domains harboring patient mutations that do not abolish F&H motif recognition, F668V and A861T[20], did not show conformational destabilization when prepared under identical conditions (Fig. 4). A recent analysis of patient fibroblasts bearing the P801L and P799L mutations showed decreased protein content when compared to wild-type control cell lines[28]. Additionally, while this manuscript was under review, a study of the interactions of the Ses proteins with OCRL also demonstrated destabilization of the full-length enzyme by missense mutations in the ASH-RhoGAP domain[21].

The A861T mutation is a splice site mutation, leading to a lack of protein product[28]. Phe668 is incorporated into a site of very high conservation in the ASH domain (Fig. 3a) that also comprises residues previously shown to affect Rab interactions[19], suggesting that its mutation to a much smaller side chain may impair Rab binding. We tested this hypothesis using a standard Rab5 GST pulldown assay and confirmed that this mutant is indeed defective in interactions with Rab5 (Fig. 5). Recently, the crystal structure of the complex of a Rab (Rab8) with the OCRL ASH domain was published[41]. The interaction surface we predicted in this study, and the importance of Phe668 for Rab recognition, is consistent between the two studies.

Given the high conservation of the F&H binding surface, it is surprising that so far no disease-causing mutation has mapped directly to this site. These mutations may exist and may be found in the future. Alternatively, direct F&H binding mutations may not be compatible with life.

DISCUSSION

The structure of the OCRL ASH-RhoGAP domain in complex with a peptide from Ses1 shows how the ASH-RhoGAP domain recognizes the F&H consensus motif and explains the tolerance for differences between the APPL1 and Ses1/2 sequences. The F&H recognition site on OCRL verifies the importance of protein folding in its formation as previously suggested[14] and shows why mutations that are spread throughout the ASH-RhoGAP domain can abolish F&H binding. Furthermore, we directly demonstrate that these mutations impair protein stability. This is in agreement with recent studies measuring OCRL protein content in patient-derived fibroblasts[28], which found that OCRL bearing missense mutations in the ASH-RhoGAP domain is not expressed at normal levels, despite the presence of normal amounts of OCRL mRNA.

Our findings support a critical role for interactions of the ASH-RhoGAP domain in the physiological function of OCRL, most likely by defining the membrane and membrane subdomains where OCRL must exercise its 5-phosphatase function. This is supported by imaging studies of OCRL proteins bearing some of these patient mutations[14,27]. Since at least one patient mutation, F668V, impairs Rab binding but preserves F&H motif binding, it would appear that the two interactions cannot compensate for each other, in spite of the fact that they partially cooperate in localizing OCRL to endosomes[27].

A striking observation is the high conservation throughout evolution of the F&H binding site in all organisms that express OCRL/INPP5B proteins, in spite of the absence of APPL1 and Ses in some of these organisms. The identification of novel interactors of this site is likely to reveal new fundamental aspects of the function of OCRL, with potential relevance for the elucidation of disease mechanisms in Lowe syndrome and Dent disease.

METHODS

Protein purification

The ASH-RhoGAP domain of OCRL (residues 536–901 of human OCRL) was expressed in BL21 DE3 pRLIP (Promega) cells as a GST-fusion (pGex6P1, GE Healthcare Lifesciences) and purified with glutathione sepharose resin (GE Healthcare Lifesciences) in 20 mM Tris pH 8, 100 mM NaCl, 10% glycerol, 1 mM EDTA, and 1 mM DTT. The GST tag was removed by addition of PreScission protease (GE Healthcare Lifesciences) directly to the column followed by incubation overnight at 4°C. The protein was then concentrated and run over a Superdex s200 gel filtration column (GE Healthcare Lifesciences) in the same buffer. The ASH-RhoGAP proteins were concentrated to 5–8 mg mL^{-1} prior to crystallization screening.

To maintain consistency with our previous publications, for SPR and stability analysis a shorter construct (than the one used for crystallography) of the ASH-RhoGAP domain was used, comprising amino acids 564–901[14], and was purified as described above. For SPR and stability analysis of patient mutations, the GST tag was not cleaved, and the protein was eluted from the column using 20 mM reduced glutathione. This was followed by overnight dialysis into the original buffer for the SPR samples or immediate inspection by colloidal coomassie staining (Invitrogen) for the analysis of stability of the patient mutation-bearing constructs.

Crystallization and data collection

Crystals of the OCRL ASH-RhoGAP domain (5 mg mL^{-1}) in complex with 500 μM Ses1 peptide were obtained by hanging drop vapor diffusion in 1.7 M Ammonium Sulfate and 0.1 M Mes pH 6.3. The rod-shaped crystals were briefly dipped in paraffin oil prior to freezing. Diffraction data was collected at the Yale University School of Medicine Macromolecular X-ray Core facility equipped with an R-Axis IV++ detector with a Rigaku MicroMax X-ray generator, and an X-stream 2000 cryogenic system. Data reduction was carried out using HKL-2000 (HKL Research, Inc.).

Structure solution and refinement

The structure was solved using molecular replacement with the previous structure of the ASH-RhoGAP domain (2qv2.pdb)[14] in which the clathrin binding loop in the RhoGAP domain had to be deleted for a correct solution to be found. The structure was solved and refined in Phenix[41] to a resolution of 2.3 Å using simulated annealing and TLS refinement. The ideal TLS groups were identified using the TLSMD server [44] with 6 TLS groups used for refinement. The final structure had 96.31% of residues in the Ramachandran favored region, and 0.34% as outliers. The final MolProbity [4546] score was 86% for similar structures in the protein data bank.

GST pulldown experiments

GST fusion proteins expressing the OCRL ASH-RhoGAP and GST fusions of the F&H peptides of APPL1 and Ses1 have been described previously[14,20]. The point mutations to introduce the substitutions W739A and D743R were made using Quikchange II XL

(Agilent). GST ASH-RhoGAP domains were purified over glutathione Sepharose (GE Healthcare Lifesciences) in 20 mM Tris pH 8, 10% (v/v) glycerol, 100 mM NaCl, 1 mM EDTA, 1 mM DTT. Rat brain lysates were prepared in the buffer described above, with the addition of Triton X-100 to 1%, and the post-nuclear supernatant applied to the fusion protein, incubated for 1 hour, washed thoroughly, and prepared for western blotting. Antibodies against APPL1 and clathrin heavy chain were described previously[14,20].

Peptide Production

Peptides comprising the APPL1 phosphorylated species were synthesized at the Yale School of Medicine W.M. Keck small-scale peptide synthesis facility. All other peptides were supplied as described previously[14,20].

Surface Plasmon Resonance

All SPR experiments were performed at the Keck Biophysics Resource facility at the Yale School of Medicine. Binding studies were performed at 25°C using a Biacore T100 optical biosensor (GE HealthCare, Biacore, Piscataway, NJ) equipped with a CM5 research-grade sensor chip coated with goat anti-GST Antibody from GST Capture Kit (Biacore, BR-1002-23). The anti-GST Ab surface was created using amine coupling and equilibrated with HBS-P+ running buffer (Biacore, BR-1006-71). The GST-OCRL ASH-RhoGAP proteins, or GST alone were captured on the anti-GST Ab surface and the binding of various peptides was monitored using a two-fold dilution series starting with either 10 or 5 μM stock (depending on expected affinity that was initially established in pilot experiments). The surfaces were regenerated by 30 s injections of glycine, pH 2.2. Each concentration was injected in duplicates and ~ 5% loss of binding capacity was observed during the second round of testing; no change in binding affinity was observed over the time of the experiment. The binding responses were double-referenced against the non-specific binding to GST alone and injections of buffer alone. The resulting sensograms were fit to a simple 1:1 binding model to determine affinity using BioEvaluation software (GE HealthCare, Biacore, Piscataway, NJ). Binding affinity was determined from binding isotherms using amplitudes observed during the steady-state phase of the binding reaction as the association and dissociation rates were too fast to be reliably determined from kinetic fits.

Live cell imaging

Cells isolated from a punch biopsy of a Lowe Syndrome patient, found to be defective for OCRL protein[37], were transfected via nucleofection (Amaxa). mTagRFP-T Ses2, mTagRFP-T Ses1, RFP-APPL1 and GFP-OCRL have been described previously[14,20]. Transfected cells were seeded on fibronectin-coated glass-bottomed 35-mm dishes (MatTek Corporation) and imaged at 0.2 Hz by spinning disk confocal (Perkin-Elmer). Images were processed using ImageJ (http://rsbweb.nih.gov/ij/). Image quantification for each cell was carried out from a single frame from live-imaged cells. For the APPL1 co-expressing cells, a total of 11 cells and 1857 individual puncta were quantitated for the $OCRL1^{WT}$ expressing condition, and 15 cells with 2492 puncta for $OCRL1^{W739A}$. For Ses2 quantification, a total of 7 cells and 2400 individual puncta ($OCRL1^{WT}$) and 17 cells with 8137 individual puncta ($OCRL1^{W739A}$) were assessed for the colocalization of Ses2 with OCRL puncta. The data are presented as the average +/− SEM, and the statistical test applied was the unpaired t-test.

Rab5 binding experiments

Full length GST-Rab5 was expressed in bacteria as a GST fusion protein. The purified protein was loaded with the indicated nucleotides as described previously[47]. Briefly, the protein was purified in 20 mM HEPES pH 7.5, 100 mM NaCl, 1 mM DTT, 1 mM $MgCl_2$ and 10 μM GDP. Nucleotide loading was accomplished by 3 rounds of incubation with the above buffer supplemented with 10 mM EDTA, 5 mM $MgCl_2$, and 1 mM nucleotide, followed by several stabilizing washes and incubations in the same buffer in the absence of EDTA. Cos-7 cells were transfected with GFP-tagged OCRL constructs, and lysates were desalted with PD10 columns (GE Healthcare Lifesciences) into nucleotide stabilizing buffer. The nucleotide-loaded Rab5 beads were incubated with the OCRL-containing lysates for 2 hours at 4°C, and samples were analyzed by western blotting using an anti-GFP antibody (Abcam 290).

Supplementary Material

Refer to Web version on PubMed Central for supplementary material.

ACKNOWLEDGMENTS

We would like to thank James Murphy at the Yale School of Medicine Macromolecular Crystallography Facility and Karin Reinisch for advice and assistance. Also we thank the Yale School of Medicine W.M. Keck small-scale peptide synthesis facility for peptide synthesis. We would also like to thank Massimiliano Stagi for computational support, and Daniel Balkin and Holger Sondermann for discussion. This work has been supported by the following funding sources: Browne-Cox postdoctoral fellowship (M.P.), NIH DK45735 and DK082700 (P.D.C.), DA018343 (E.F.S. and P.D.C.), and grants from the Lowe Syndrome Association (P.D.C.) and the Lowe Syndrome Trust (P.D.C. and L.S.). The Biacore T100 instrumentation, as well as the size exclusion chromatography and light scattering instrumentation (SEC/LS system), were supported by NIH grants 1S10RR026992 and 1S10RR023748, respectively.

REFERENCES

1. Attree O, et al. The Lowe's oculocerebrorenal syndrome gene encodes a protein highly homologous to inositol polyphosphate-5-phosphatase. Nature. 1992; 358:239–242. [PubMed: 1321346]
2. Hoopes RRJ, et al. Dent Disease with mutations in OCRL1. Am J Hum Genet. 2005; 76:260–267. [PubMed: 15627218]
3. Bockenhauer D, et al. Renal phenotype in Lowe Syndrome: a selective proximal tubular dysfunction. Clin J Am Soc Nephrol. 2008; 3:1430–1436. [PubMed: 18480301]
4. Delleman JW, Bleeker-Wagemakers EM, van Veelen AW. Opacities of the lens indicating carrier status in the oculo-cerebro-renal (Lowe) syndrome. J Pediatr Ophthalmol. 1977; 14:205–212. [PubMed: 894443]
5. Kenworthy L, Charnas L. Evidence for a discrete behavioral phenotype in the oculocerebrorenal syndrome of Lowe. Am J Med Genet. 1995; 59:283–290. [PubMed: 8599350]
6. Schurman SJ, Scheinman SJ. Inherited cerebrorenal syndromes. Nat Rev Nephrol. 2009; 5:529–538. [PubMed: 19701229]
7. Bokenkamp A, et al. Dent-2 disease: a mild variant of Lowe syndrome. J Pediatr. 2009; 155:94–99. [PubMed: 19559295]
8. Shrimpton AE, et al. OCRL1 mutations in Dent 2 patients suggest a mechanism for phenotypic variability. Nephron Physiol. 2009; 112:p27–p36. [PubMed: 19390221]
9. Bothwell SP, Farber LW, Hoagland A, Nussbaum RL. Species-specific difference in expression and splice-site choice in Inpp5b, an inositol polyphosphate 5-phosphatase paralogous to the enzyme deficient in Lowe Syndrome. Mamm. Genome. 2010; 21:458–466. [PubMed: 20872266]

10. Janne PA, et al. Functional overlap between murine Inpp5b and Ocrl1 may explain why deficiency of the murine ortholog for OCRL1 does not cause Lowe syndrome in mice. J Clin Invest. 1998; 101:2042–2053. [PubMed: 9593760]
11. Dressman MA, Olivos-Glander IM, Nussbaum RL, Suchy SF. Ocrl1, a PtdIns(4,5)P(2) 5-phosphatase, is localized to the trans-Golgi network of fibroblasts and epithelial cells. J Histochem Cytochem. 2000; 48:179–190. [PubMed: 10639484]
12. Olivos-Glander IM, Janne PA, Nussbaum RL. The oculocerebrorenal syndrome gene product is a 105-kD protein localized to the Golgi complex. Am J Hum Genet. 1995; 57:817–823. [PubMed: 7573041]
13. Suchy SF, Olivos-Glander IM, Nussabaum RL. Lowe syndrome, a deficiency of phosphatidylinositol 4,5-bisphosphate 5-phosphatase in the Golgi apparatus. Hum Mol Genet. 1995; 4:2245–2250. [PubMed: 8634694]
14. Erdmann KS, et al. A role of the Lowe syndrome protein OCRL in early steps of the endocytic pathway. Dev. Cell. 2007; 13:377–390. [PubMed: 17765681]
15. Mao Y, et al. A PH domain within OCRL bridges clathrin-mediated membrane trafficking to phosphoinositide metabolism. EMBO J. 2009; 28:1831–1842. [PubMed: 19536138]
16. Ungewickell A, Ward ME, Ungewickell E, Majerus PW. The inositol polyphosphate 5-phosphatase Ocrl associates with endosomes that are partially coated with clathrin. Proc Natl Acad Sci USA. 2004; 101:13501–13506. [PubMed: 15353600]
17. Faucherre A, et al. Lowe syndrome protein OCRL1 interacts with Rac GTPase in the trans-Golgi network. Hum Mol Genet. 2003; 12:2449–2456. [PubMed: 12915445]
18. Fukuda M, Kanno E, Ishibashi K, Itoh T. Large scale screening for novel rab effectors reveals unexpected broad Rab binding specificity. Mol Cell Proteomics. 2008; 7:1031–1042. [PubMed: 18256213]
19. Hyvola N, et al. Membrane targeting and activation of the Lowe syndrome protein OCRL1 by rab GTPases. EMBO J. 2006; 25:3750–3761. [PubMed: 16902405]
20. Swan LE, Tomasini L, Pirruccello M, Lunardi J, de Camilli P. Two closely related endocytic proteins that share a common OCRL-binding motif with APPL1. Proc Natl Acad Sci USA. 2010; 107:3511–3516. [PubMed: 20133602]
21. Noakes CJ, Lee G, Lowe M. The PH domain proteins IPIP27A and B link OCRL1 to receptor recycling in the endocytic pathway. Mol Biol Cell. 2011
22. Zoncu R, et al. A phosphoinositide switch controls the maturation and signaling properties of APPL endosomes. Cell. 2009; 136:1110–1121. [PubMed: 19303853]
23. Miaczynska M, et al. APPL proteins link Rab5 to nuclear signal transduction via an endosomal compartment. Cell. 2004; 116:445–456. [PubMed: 15016378]
24. National Human Genome Research Institute Database of the OCRL1 Mutations Causing Lowe Syndrome. 2010
25. Monnier N, Satre V, Lerouge E, Berthoin F, Lunardi J. OCRL1 mutation analysis in French Lowe syndrome patients: implications for molecular diagnosis strategy and genetic counseling. Hum Mutat. 2000; 16:157–165. [PubMed: 10923037]
26. Addis M, Loi M, Lepiani C, Cau M, Melis MA. OCRL mutation analysis in Italian patients with Lowe syndrome. Hum Mutat. 2004; 23:524–525. [PubMed: 15108291]
27. McCrea HJ, et al. All known patient mutations in the ASH-RhoGAP domains of OCRL affect targeting and APPL1 binding. Biochem Biophys Res Commun. 2008; 369:493–499. [PubMed: 18307981]
28. Hichri H, et al. From Lowe syndrome to Dent disease: correlations between mutations of the OCRL1 gene and clinical and biochemical phenotypes. Hum Mutat. 2010
29. Yuksel A, Karaca E, Albayram MS. Magnetic resonance imaging, magnetic resonance spectroscopy, and facial dysmorphism in a case of Lowe syndrome with novel OCRL1 gene mutation. J Child Neurol. 2009; 24:93–96. [PubMed: 19168822]
30. Tosetto E, et al. Locus heterogeneity of Dent's disease: OCRL1 and TMEM27 genes in patients with no CLCN5 mutations. Pediatr. Nephrol. 2009; 24:1967–1973. [PubMed: 19582483]

31. Kawano T, Indo Y, Nakazato H, Shimadzu M, Matsuda I. Oculocerebrorenal syndrome of Lowe: three mutations in the OCRL1 gene derived from three patients with different phenotypes. Am J Med Genet. 1998; 77:348–355. [PubMed: 9632163]
32. Lichter-Konecki U, Farber LW, Cronin JS, Suchy SF, Nussbaum RL. The effect of missense mutations in the RhoGAP-homology domain on ocrl1 function. Mol Genet Metab. 2006; 89:121–128. [PubMed: 16777452]
33. Lin T, et al. Spectrum of mutations in the OCRL1 gene in the Lowe oculocerebrorenal syndrome. Am J Hum Genet. 1997; 60:1384–1388. [PubMed: 9199559]
34. Holm L, Rosenstrom P. Dali server: conservation mapping in 3D. Nucleic Acids Res. 2010; 38(Suppl):W545–W549. [PubMed: 20457744]
35. Kaiser SE, et al. Structural basis of FFAT motif-mediated ER targeting. Structure. 2005; 13:1035–1045. [PubMed: 16004875]
36. Gant-Branum RL, Broussard JA, Mahsut A, Webb DJ, McLean JA. Identification of phosphorylation sites within the signaling adaptor APPL1 by mass spectrometry. J Proteome Res. 2010; 9:1541–1548. [PubMed: 20095645]
37. Wenk MR, et al. Phosphoinositide profiling in complex lipid mixtures using electrospray ionization mass spectrometry. Nat Biotechnol. 2003; 21:813–817. [PubMed: 12808461]
38. Zhu G, et al. Structure of the APPL1 BAR-PH domain and characterization of its interaction with Rab5. EMBO J. 2007; 26:3484–3493. [PubMed: 17581628]
39. Ponting CP. A novel domain suggests a ciliary function for ASPM, a brain size determining gene. Bioinformatics. 2006; 22:1031–1035. [PubMed: 16443634]
40. Nassar N, Hoffman GR, Manor D, Clardy JC, Cerione RA. Structures of Cdc42 bound to the active and catalytically compromised forms of Cdc42GAP. Nat Struct Biol. 1998; 5:1047–1052. [PubMed: 9846874]
41. Hou X, et al. A structural basis for Lowe syndrome caused by mutations in the Rab-binding domain of OCRL1. EMBO J. 2011
42. Schrödinger. LLC The PyMOL Molecular Graphics System. 2010
43. Deprez C, et al. Solution structure of the E.coli TolA C-terminal domain reveals conformational changes upon binding to the phage g3p N-terminal domain. J. Mol. Biol. 2005; 346:1047–1057. [PubMed: 15701516]
44. Painter J, Merritt EA. TLSMDweb server for the generation of multi-group TLS models. J Appl Crystallogr. 2006; 39:109–111.
45. Chen VB, et al. MolProbity: all-atom structure validation for macromolecular crystallography. Acta Crystallogr D Biol Crystallogr. 2010; 66:12–21. [PubMed: 20057044]
46. Davis IW, et al. MolProbity: all-atom contacts and structure validation for proteins and nucleic acids. Nucleic Acids Res. 2007; 35:W375–W383. [PubMed: 17452350]
47. Christoforidis S, Zerial M. Purification and identification of novel Rab effectors using affinity chromatography. Methods. 2000; 20:403–410. [PubMed: 10720461]

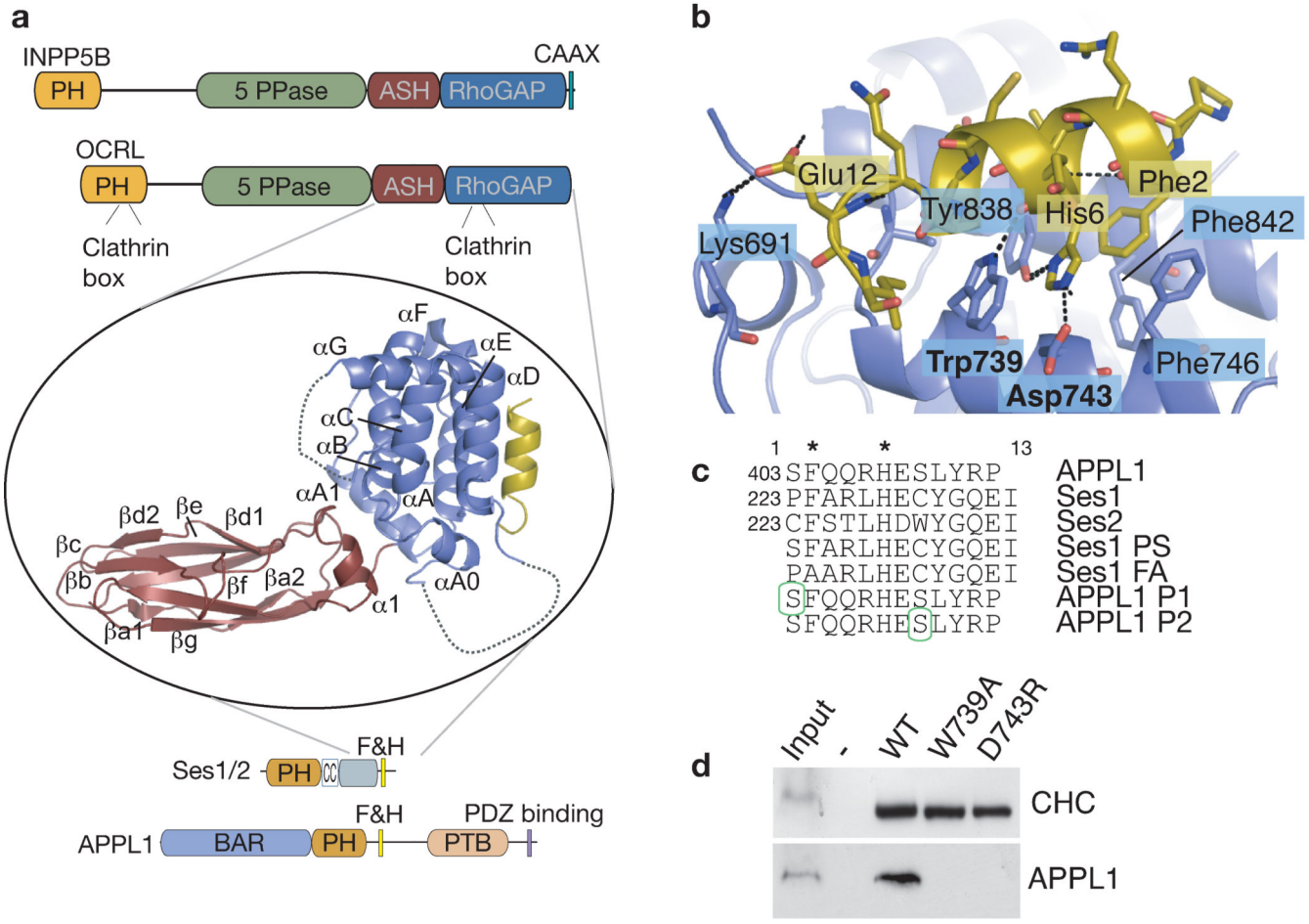

Figure 1.

Domain structures of INPP5B and OCRL and their F&H motif-containing interactors, and the crystal structure of the human ASH-RhoGAP domain in complex with the F&H peptide from human Ses1. (a) The ASH domain is colored in red, the RhoGAP domain in blue, and the Ses1 F&H peptide in yellow. Molecular graphics for this and all subsequent figures were generated with Pymol[42]. (b) Close-up view of the interface between the F&H peptide (yellow) and the RhoGAP domain (blue). (c) F&H peptide sequences used in this study. Phosphoserine residues are indicated in green. (d) GST-ASH-RhoGAP constructs of OCRL were assayed for binding to APPL1 from rat brain homogenate. The GST negative control is marked as a -, and the OCRL constructs are either wild-type (WT), or mutated in the F&H binding site (W739A and D743R). As predicted, the mutants disrupt binding to APPL1, without affecting binding to clathrin heavy chain (CHC).

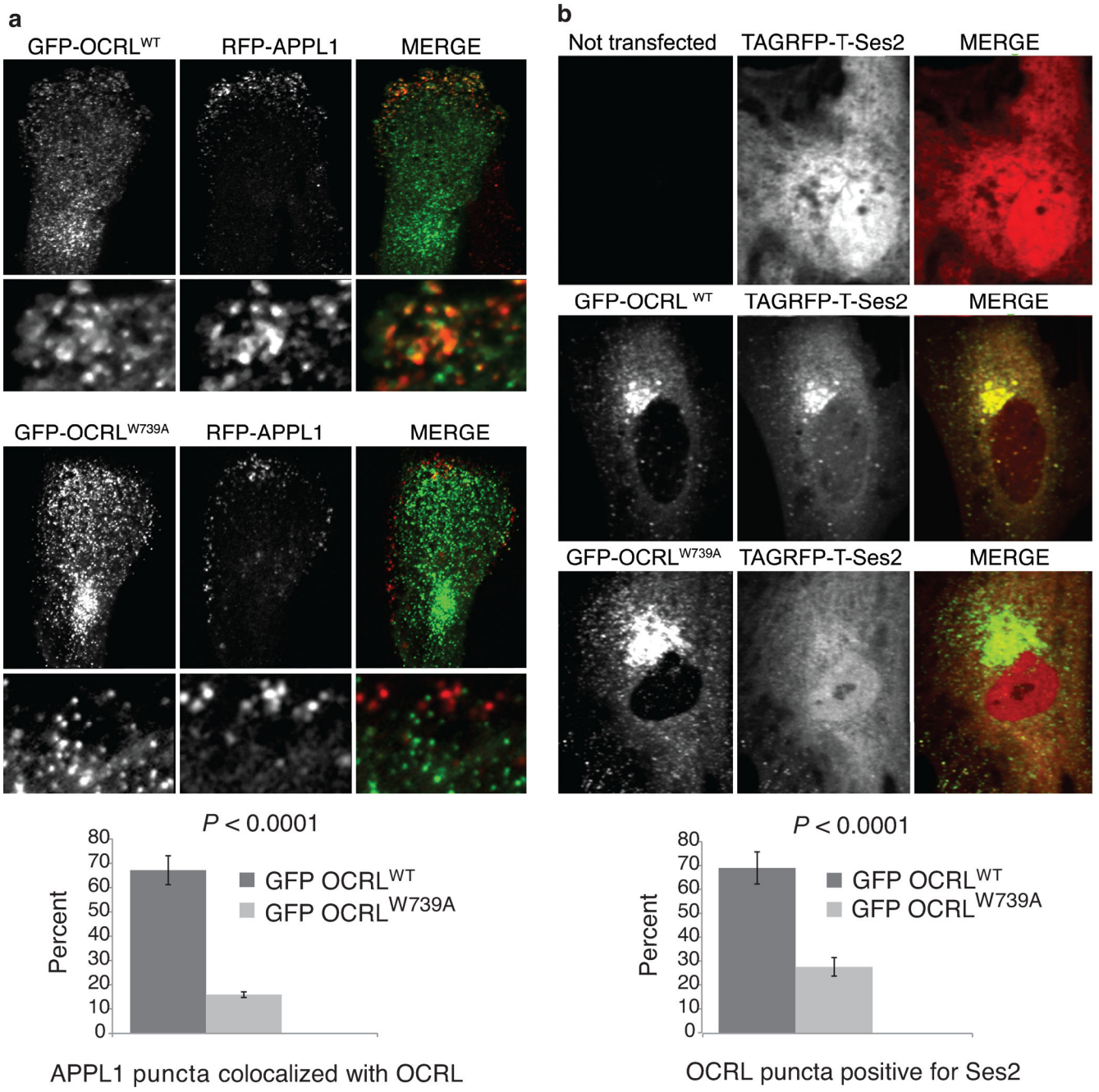

Figure 2.

Mutation of the F&H binding site in OCRL disrupts its colocalization with F&H motif-containing proteins. Colocalization of exogenously expressed OCRL and F&H motif-containing proteins was assessed in human fibroblasts derived from a patient with Lowe Syndrome [37]. Images are shown in the top panels, with quantitation below. (a) Mutation of the F&H interface (W739A) disrupts colocalization of RFP-APPL1 and GFP-OCRL on individual endosomes, although the overall localization of the two proteins is not compromised. Quantification of the colocalization of APPL1 with OCRL^{WT} and

OCRL^{W739A} is expressed as the percentage of APPL1 colocalizing with the OCRL protein. (b) mTagRFP-T-Ses2 expressed in the absence of co-transfected OCRL is primarily cytosolic. When co-transfected with GFP-OCRL^{WT}, mTagRFP-T-Ses2 colocalizes with this protein on endosomes and in the Golgi complex area, but this colocalization is disrupted by the W739A mutation in OCRL. The quantification of colocalization is expressed as a function of the colocalization in well-defined puncta, as the main result of the mutation is a diffuse signal of the Ses2 protein, and errors are the SEM.

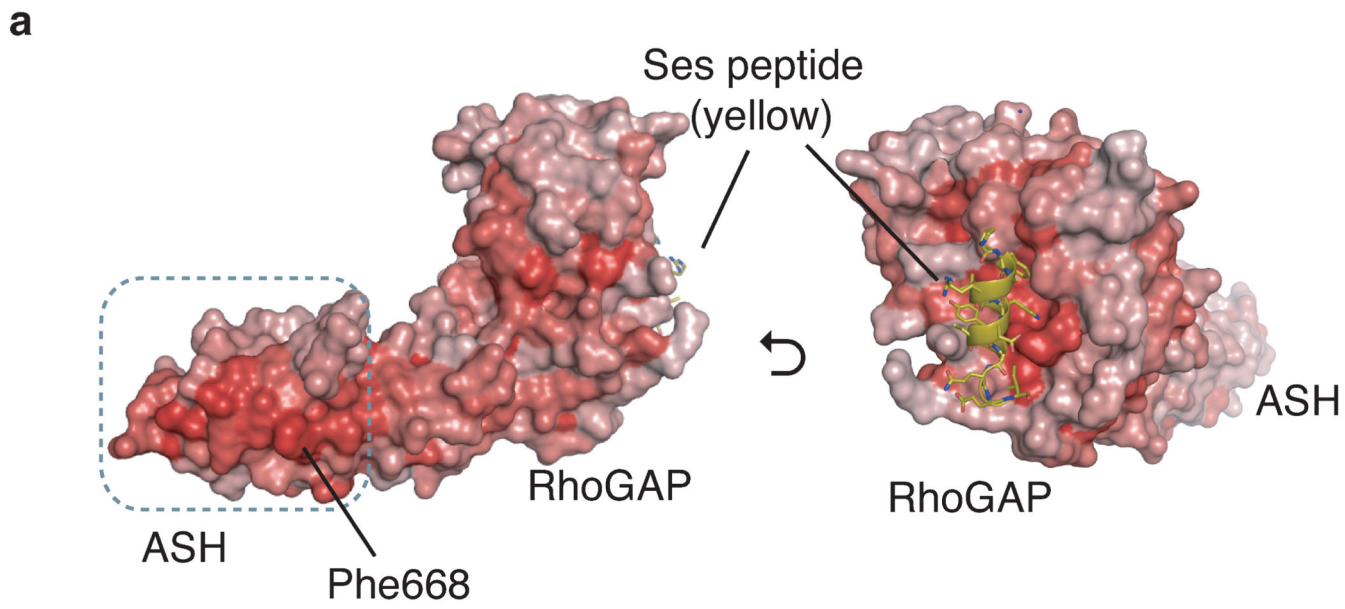

b

Homo sapiens OCRL	EGASERPLQVPKEIWLLVDHLFKY
Homo sapiens INPP5B	GSQLDSPMEIPKELWMMVDYLYRN
Macaca mulatta OCRL	EGASERPLQVPKEIWLLVDHLFKY
Macaca mulatta INPP5B	GSQLESPMEIPKELWMMVDYLYRN
Mus musculus OCRL	EGTSERPLQVPKEIWLLVDHLFKY
Mus musculus INPP5B	RSQLENPMEIPKELWMMVDYLYRN
Gallus gallus	EDASEMPLQMPKEIWLLVDHLYKH
Danio rerio	AGTEDKPLKIPKEVWLLVNHLYTK
Dictyostelium discoideum	-----KKLSIPKELWRIIDYIYYN
Caenorhabditis elegans	SLSDNCPPNVPRVIYRLVMALRTR
Trypanosoma brucei	RRSGGCMPQIPKELWYLCEAIYER

Figure 3.

Conserved surfaces of the ASH-RhoGAP domain map to the F&H interaction and potential Rab interaction surfaces. (a) Surface representation is colored by degree of conservation with the darker colors indicating the most conservation. Images were generated using PROTSKIN[43]. (b) Sequence alignment highlighting the conservation of the major residues responsible for recognition of the F&H motif. Accession codes for sequences used in the alignment are listed in Supplementary information.

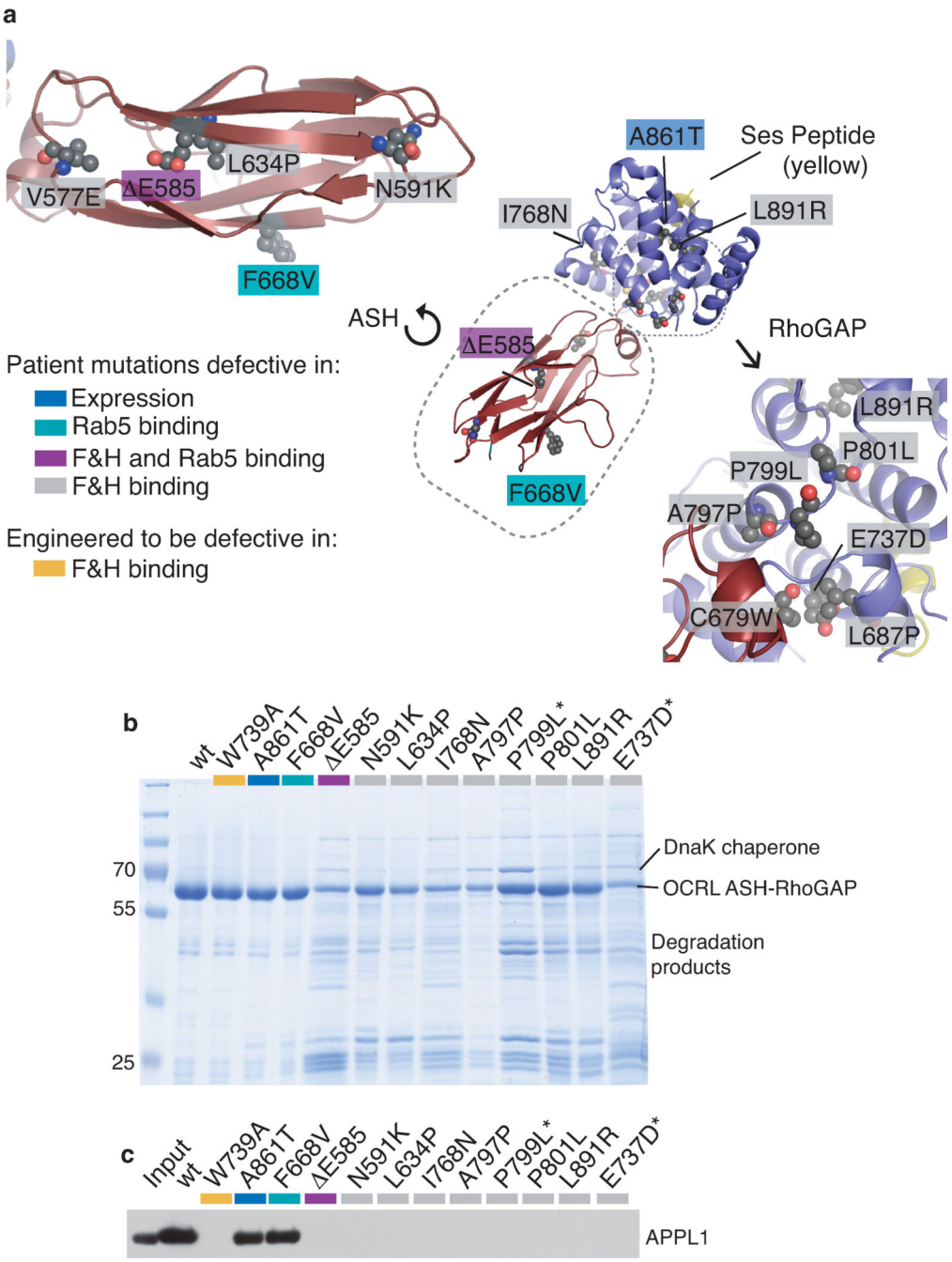

Figure 4.

Patient mutations affecting F&H binding are global folding mutations. Patient mutations are represented in all structures as spheres. (a) The mapping of the patient missense mutations onto the ASH-RhoGAP structure, with two mutation networks expanded, one in the ASH domain and the other in the RhoGAP domain. (b) F&H binding is disrupted due to destabilization of OCRL. Inspection of a coomassie-stained gel shows significant degradation as well as the co-purification of a DnaK chaperone for mutants that display a lack of F&H binding. This destabilization is not seen in our designed F&H-binding mutation

(W739A), a Rab5-defective mutant (F668V), or a splice-site mutation that results in a lack of expressed protein (A861T). Patient mutations which give rise to Dent 2 disease are indicated by an asterisk. (c) The GST-ASH-RhoGAP OCRL constructs in panel b were assessed for APPL1 binding using a GST pulldown assay from rat brain followed by western blot for APPL1.

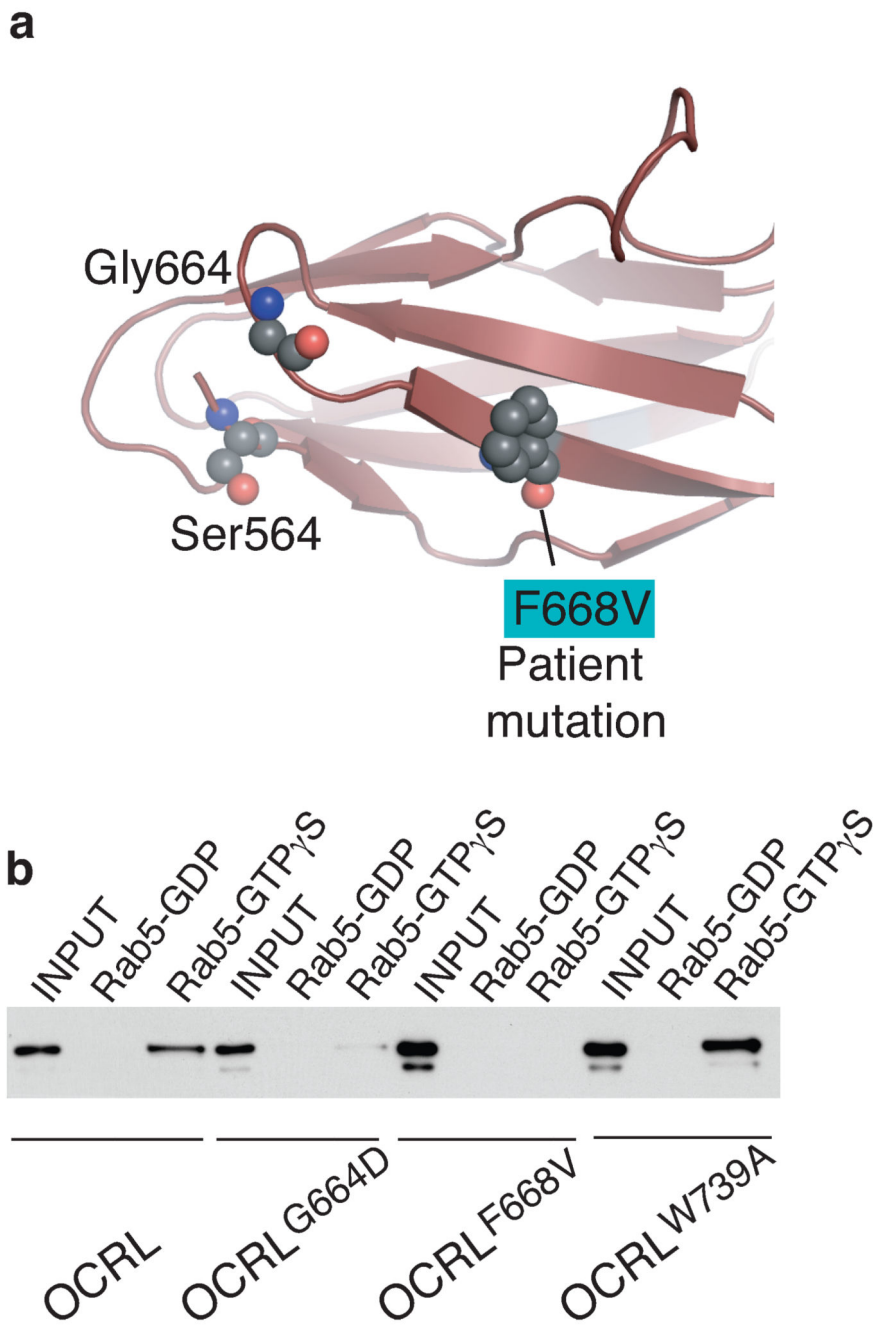

Figure 5.

Characterization of a Rab5 binding-deficient mutation. (a) The residues shown to be important for Rab binding both in previous studies[19], as well as in this one (Phe668), are represented as gray spheres. (b) Pull-downs using nucleotide-loaded Rab5 as bait for over-expressed OCRL constructs show that the GTPγS-dependent interaction between Rab5 and OCRL is perturbed by the F668V mutation, while not affected by mutation of the F&H recognition site.

Table 1

X-ray data collection and refinement statistics.

Data collection	
Space group	$P3_121$
Cell dimensions	
a, *b*, *c* (Å)	73.48, 73.48, 145.29
α, β, γ (°)	90, 90, 120
Resolution (Å)	24.05(2.3) *
R_{sym}	7.7(67.4)
$I / \sigma I$	15(2.5)
Completeness (%)	94.8(93.1)
Redundancy	9.2(9.2)
Refinement	
Resolution (Å)	2.3
No. reflections	177,198
R_{work} / R_{free}	19.5/23.8
No. atoms	
Protein	2508
Water	123
B-factors	
Protein	48.9
Solvent	42.5
R.m.s. deviations	
Bond lengths (Å)	0.006
Bond angles (°)	0.9

* Highest-resolution shell.

Table 2

Summary of binding affinities measured by surface plasmon resonance (SPR). The binding affinities between recombinant OCRL ASH-RhoGAP domain constructs and peptides comprising the F&H motif of various proteins is shown. The sequences of the peptides are shown in Figure 1c. Due to the slow loss of GST-fusion proteins, the K_d estimates were higher in SPR than in the previous ITC studies[14,20] by a factor of approximately 4, however, the trends in affinities remained consistent. NB indicates no binding was detected. Representative traces can be found in the supplementary information.

	APPL1	Ses1	Ses 2	Ses1 FA	Ses1 PS	APPL1 P1	APPL1 P2
OCRL^{WT}	43.1 +/− 0.4	5.8 +/− 0.3	2.5 +/− 0.4	NB	3.0 +/− 0.2	NB	NB
OCRL^{W739A}	NB	NB	NB	NB	NB	NB	NB